

# Block copolymer supramolecular assemblies: switching, fine structure and applications

*We have investigated formation and fine structure of thin films of assembly of poly(styrene-block-4-vinylpyridine) copolymer with -2-(4'-hydroxybenzeneazo)benzoic acid (PS-PVP + HABA) using the combination of atomic force microscopy (AFM), ellipsometry, X-ray reflectivity, GISAXS (grazing incidence small-angle X-ray scattering), XPS (photoelectron spectroscopy) and XPEEM (X-ray photoemission electron microscopy). The films consist of cylindrical nano-domains formed by PVP + HABA associates surrounded by PS matrix. Alignment of the domains can be switched upon exposure to vapors of different solvents from the parallel to the perpendicular orientation and vice versa in respect to the surface plane. Swelling in 1,4-dioxane leads the system from the cylindrical to the spherical morphology. The solvent evaporation results in a shrinkage of the matrix in the vertical direction and subsequent merging of the spheres into the perpendicularly aligned cylinders. The cylinders form regular hexagonal lattice with the spatial period of 25.5 nm. On the other hand, vapors of chloroform induce the in-plane alignment. The films consist of parallel layers of the cylinders separated by PS matrix and demonstrate the fingerprint-like structure. The nano-cylinders of PVP + HABA are packed into distorted hexagonal lattice exhibiting 31 nm in-plane and 17 nm vertical periodicity. In the both cases, thin wetting layer is found at the polymer/substrate interface. The free surface is enriched with PS.*

*We demonstrate several principal possibilities of use of the templates. Loading of the templates with magnetic and non-magnetic metals and electro-conductive polymers is performed either by sputter-coating or electrochemical deposition.*

## Introduction

The last two decades demonstrate tremendous increase of interest to investigation of self-organization and self-assembly phenomena in soft matter. According to definition by G. Whitesides, self-assembly is "the aggregation of molecular moieties into more ordered structures that are thermodynamically stable and involve non-covalent bonds. Crystallization is an example of such self-assembly. Self-assembly is used to build nano-structures such as inorganic clusters and lattices, nano-tubes and channels, host-guest complexes, monolayers, hydrogen-bonded networks and systems of intertwined molecules" [1,2]. Thin films of block copolymers are one of the most prominent examples of systems capable to self-assembly. They are of special interest because of nanometer ordering scale of these systems [3]. The increasing growth of number of publications in this field is demonstrated in Fig. 1. We narrowed our search by two keywords: *block copolymer* and *thin film*. More than 100 scientific papers published in the year 2003 in refereed journals over the wide world and the dynamics traced back to 20 years reflects sufficient interest to this topic. This dynamics results from growing expectations for possible applications of well ordered nanometer scale block copolymer films for nano-electronics, photovoltaic and data storage devices, flexible electronic elements, nano-lithography etc.

## Keywords

block copolymers  
supramolecular assembly  
molecular assembly  
self-organization  
thin films

## Bearbeiter

A. Sydorenko  
I. Tokarev  
R. Krenek  
S. Minko  
M. Stamm

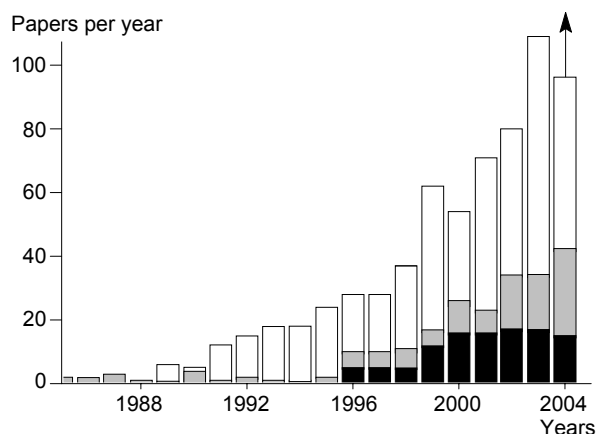
## Förderer

Bundesministerium für Bildung und  
Forschung  
Deutsche Forschungsgemeinschaft

## Kooperation

Dr. Vera Cimrova  
Institute of Macromolecular  
Chemistry, Prague, Czech Republic  
Prof. Dieter Schmeisser  
Brandenburg Technical University  
Cottbus  
Dr. Peter Müller-Buschbaum  
Technical University of Munich

Fig. 1:  
Dynamics of publications in the topic defined as block copolymer and thin film published over wide world (□), by Wiley Interscience (▨) and American Chemical Society (■). It is expected more papers in the year 2004. Based on the search with SciFinder



### Selection of the materials and investigation of formation and microphase separation of block copolymer supramolecular assemblies (BCA)

On the first stage of the investigation we performed thorough search of the materials (block copolymers and additives) which satisfy to the following criteria: selective hydrogen bonding between one of the blocks of BC and additive, strong microphase separation, easy extraction of the additive, ability to form thin films, easy to visualize. We selected well-known block copolymer recently used by Ikkala for synthesis and investigations of supramolecular comb copolymer-like systems, i.e. poly(styrene-*block*-4-vinylpyridine) (PS-PVP) [4-7]. We used two samples of PS-PVP of different molecular weight:  $M_n^{PS} = 35\,500\text{ g}\cdot\text{mol}^{-1}$ ,  $M_n^{PVP} = 3\,680\text{ g}\cdot\text{mol}^{-1}$ , denoted further as BC1, and  $M_n^{PS} = 32\,900\text{ g}\cdot\text{mol}^{-1}$ ,  $M_n^{PVP} = 8\,080\text{ g}\cdot\text{mol}^{-1}$ , denoted further as BC2. As an additive we have chosen 2-(4'-hydroxybenzeneazo)benzoic acid (HABA) which possesses two polar groups capable to form hydrogen bonds with PVP block and azobenzene group with high molar extinction (azo-dye). The samples of equimolar HABA (in respect to PVP content) of BC1 + HABA and BC2 + HABA were investigated with Fourier Transform infrared spectroscopy (FTIR), UV/Vis spectroscopy and small-angle X-ray scattering (SAXS) before and after HABA extraction. FTIR spectra showed formation of strong hydrogen bonds between HABA and nitrogen of PVP block. UV/Vis spectroscopy gave strong evidence for H-aggregation of HABA (parallel face-to-face, according to the molecular exciton model). Moreover, UV/Vis measurements showed complete extraction of HABA with methanol in 2 min. SAXS of BC1+HABA and BC2+HABA demonstrated typical scattering patterns characteristic for BC with the periodicity of 25.5 nm and 31 nm, respectively. However, extraction of HABA results in drastic increase of the electron density contrast and, thus, sufficient increase of scattering signal. Noteworthy, the periodicity of washed samples was identical to the samples as prepared. The results obtained for BC1 + HABA and BC2 + HABA were similar to those found for PS-PVP with *n*-pentadecylphenol as reported by Ikkala [5]. Therefore, we focused our next steps on the investigations of morphology and orientation of BCA in thin films. The general concept of the BCA approach is shown in the Fig. 2.

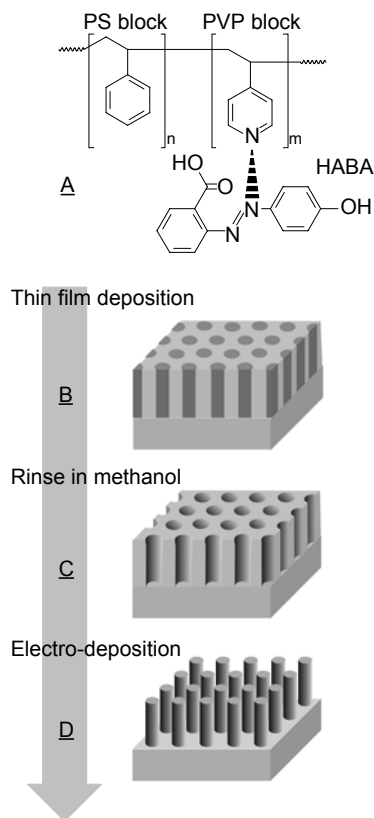


Fig. 2:  
General concept of the use of block copolymer assembly approach for nano-templating

### Thin films of cylinder forming assembly (BC1)

BCA films on silicon wafers were prepared by either spin- or dip-coating. In optical microscope the polymer films with the thickness ranging from 20 to 100 nm (ellipsometry) are macroscopically and microscopically smooth and show no signs of HABA phase separation, such as crystals or stains. It suggests that HABA molecules are associated with PVP blocks building comb-like polymer chains. The AFM scratch test gives the same film thickness as ellipsometry if the BCA film is modeled as a layer with apparent refractive index  $n = 1.63$ . Such an elevated value of apparent refractive index as compared to that for PS-PVP (1.59) is attributed to significant fraction of HABA.

The detail investigation of BCA films with AFM shows the dependence of the morphology on the deposition conditions. BCA films deposited from chloroform solution demonstrate the terrace formation. The films are very smooth inside of the terraces with rms roughness of about 0.3 nm for  $1 \times 1 \mu\text{m}^2$  lateral scale. In contrast, BCA films deposited from 1,4-dioxane are flat and featureless. The rms roughness is 0.15 nm as measured on  $1 \times 1 \mu\text{m}^2$  lateral scale. We did not visualize the fine structure of the materials because of poor contrast between mechanical behavior of PS and PVP+HABA domains in the film.

As expected, methanol destroys supramolecular assemblies and removes selectively HABA from BCA leaving cylindrical cavities in the film. The AFM scratch test showed no difference in film thickness before and after washing. It gives evidence that almost all HABA is located in PVP domains because the thickness of the PS matrix remains unchanged. Ellipsometric data for the same film thickness were fitted with the apparent refractive index  $n = 1.50 \pm 0.01$ . Such decrease of  $n$  from 1.63 for BCA film (before washing) to 1.5 (after washing) is effected by the formation of porous morphology of the film due to the elimination of HABA.

Note that the obtained  $n$  value is much lower than  $n = 1.59$  for the PS-PVP reference film which gives additional evidence for the formation of membrane with porous morphology. The estimated volume fraction of the pores in the membrane ( $n_{PS} = n_{PVP} = 1.59$ ) is in good agreement with the concentration of HABA in the initial mixture (17.8 %). The rinsing with methanol develops the fine structure of the films clearly observed with AFM. The film deposited from chloroform shows well aligned stripes which can be assigned as  $C_{\parallel}$  cylindrical domains.

The film deposited from 1,4-dioxane and washed with methanol demonstrates caves of about 9 nm in diameter which are projection of  $C_{\perp}$  domains (channels) with periodicity of about  $25 \pm 1$  nm (Fig. 3). The center-center distance distribution found for the membranes prepared from the *as deposited* films is comparable with the distribution of an optimized PS-PVP film obtained by the *neutral surface* approach. We observed the same level of order for different film thickness ranging from 20 to 100 nm. X-ray reflectivity gives strong evidence for formation of  $C_{\perp}$  and  $C_{\parallel}$  patterns after swelling in 1,4-dioxane and chloroform, respectively. XPEEM shows completeness of the terraces in the case of  $C_{\parallel}$  and presence of PS block at the polymer/air interface. It is noteworthy, that the same behavior was found for substrates of *different chemical compositions*, for example PS brush, gold, ITO-glass, and Ni. Thus, the film morphology is insensitive to the substrate surface nature.

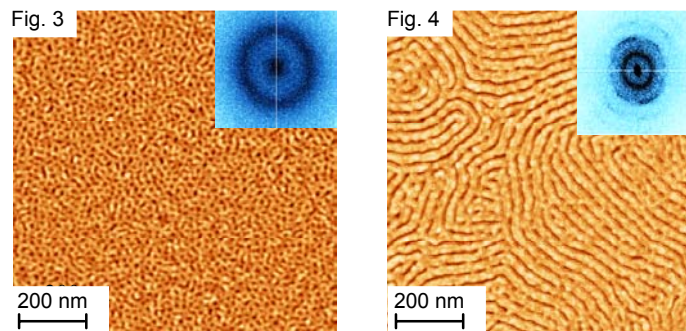
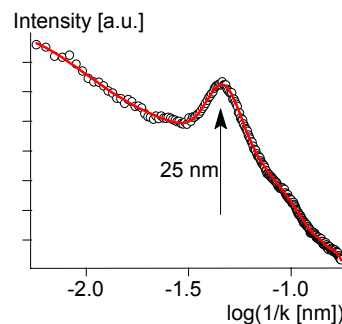


Fig. 3:  
AFM image of BCA deposited from 1,4-dioxane ( $C_{\perp}$  pattern) with the corresponding FFT (Fast Fourier Transform) image and power spectral density plot.  
 $k$  = wave number

Fig. 4:  
AFM image of BCA after swelling in chloroform ( $C_{\parallel}$  pattern)



Alignment of cylindrical domains in BCA films can be easily changed with appropriate solvent, for example, upon annealing of the 60 nm thick film deposited from 1,4-dioxane ( $C_{\perp}$  pattern) in saturated vapor of chloroform for 30 min at room temperature. Once the sample was removed from the chamber, it dried in about 1 sec. Then we rinsed it with methanol. The film reveals the characteristic  $C_{\parallel}$  morphology similar to the morphology obtained directly after deposition from chloroform solution (Fig. 4). Oppositely, BCA films deposited from chloroform with  $C_{\parallel}$  alignment were re-oriented into hexagonal  $C_{\perp}$  morphology by annealing in 1,4-dioxane saturated vapor atmosphere for 30 min at room temperature. Moreover, swelling of the BCA film in 1,4-dioxane vapor results in a significant increase of order (Fig. 5).

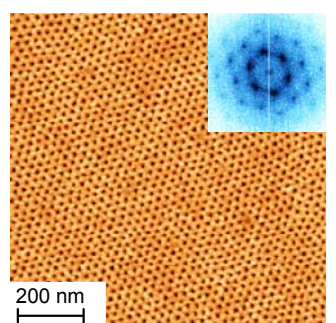


Fig. 5:  
AFM image of BCA deposited after swelling up to 2.5 ratio in 1,4-dioxane ( $C_{\perp}$  pattern) with the corresponding FFT image and power spectral density plot

The center-center distance distribution is very narrow (standard deviation 9 %). Six sharp first order peaks and the presence of higher order reflections are clearly seen on the FFT image demonstrating the almost perfect hexagonal order spreading over area of 0.2 up to  $2 \mu\text{m}^2$ . GISAXS out-of-plane scattering gives direct evidence for the realignment. We assume that the well ordered structure is promoted by aggregation of HABA molecules. The realignment occurring in BCA is reversible, relatively fast, and can be repeated several times for not rinsed films. Kinetics of the realignment was monitored by analyzing morphology of the films as a function of time and swelling degree (evaluated with ellipsometry).

We found out that the realignment began upon exposure to saturated vapor of solvent if the swelling approached 2.5 times increase of film thickness (in our experiments this swelling degree was observed in 10 min). Then the completed realignment was approached in about 10 min. Very similar kinetics was observed for different solvents.

The experiments were performed in different solvents and we found out that the stability of the  $C_{\perp}$  alignment increased with the increased reactivity of the solvent in formation of hydrogen bonds. For example, the  $C_{\parallel}$  alignment was found in toluene and chloroform. The shape memory alloy (SMA) films deposited from THF exhibit a co-existence of  $C_{\parallel}$  and  $C_{\perp}$  structures, while in 1,4-dioxane the  $C_{\perp}$  structure is stable. Solvent evaporation drives the BCA structure to adopt the perpendicular orientation. 1,4-dioxane is a solvent selective for the PS matrix. Swelling in 1,4-dioxane leads the system from cylindrical to spherical morphology. Solvent evaporation results in a shrinkage of the matrix in the vertical direction and subsequently merges the spheres into the vertical cylinders.

On the other hand, considering the above mentioned behavior and the structure of the SMA film we may speculate that the reversible and dynamic supramolecular aggregation between PVP and HABA via hydrogen bonds may introduce the mechanism of self-adapting of the interface composition. Redistribution of HABA molecules between bulk and interface occurs to approach a minimum interface energy for the particular alignment and environment, making the morphology insensitive to the confining surface. Solvent plays

a very important role competing with PVP for HABA molecules so that a subtle interplay between HABA-PVP-solvent interface interactions may result in conditions to switch in the mechanism as it proved by the FTIR spectra. This mechanism helps to overcome surface dominant alignment as compared to BC films. The detail investigation of the mechanism requires consideration of many parameters and it is out of the focus of this paper. The prevalent role of HABA is the subject of our future investigations.

### Thin films of lamella forming assembly (BC2)

Similarly to BC1 based assembly, BC2 + HABA assembly was synthesized. Thin films of the BCA demonstrate the lamellar structure as revealed by ellipsometry, AFM and X-ray reflectivity. As well, lamellar BCA shows strong tendency to realignment (switching) upon vapor annealing depending on the solvent used. Chloroform vapors induce parallel alignment with the typical for parallel alignment terrace formation (Fig. 6). The height of the terraces amounts to 31 nm. Extraction of HABA results in sufficient decrease of the terrace height down to 21 nm, which correspond to the amount of HABA in the assembly (30 % by volume). In contrast, swelling in 1,4-dioxane results in the fingerprint-like pattern with the periodicity of 31 nm. After HABA extraction the groves are clearly seen. Ellipsometry of the washed films of the BCA reveals sufficiently lower refractive index of about 1.42; the index corresponds to about 30 % pore fraction according to the Bruggeman's equation. Both ellipsometry and AFM give evidence of switchable lamellar morphology of the BC2+HABA assembly.

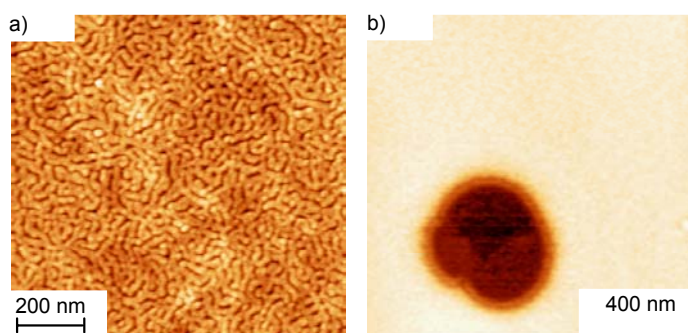


Fig. 6: Solvent induced switching of the orientation of lamella forming BCA as evidenced by AFM: after annealing in 1,4-dioxane (a,  $L \perp$  pattern) and chloroform (b,  $L \parallel$  pattern)

### Loading of nano-templates

It is noteworthy, that the walls of the channels formed after rinsing with methanol are constituted from the brush of PVP chains. The free space left by HABA molecules can be reversibly occupied by swollen PVP chains upon exposure the membrane to selective solvent or acidic aqueous solution. Thus, the fabricated membranes belong to the class of smart membranes with uniform reactive channels of a narrow distribution in size.

The nano-membrane prepared by rinsing in methanol of the SMA film in the  $C \perp$  orientation on the gold coated silicon substrate was filled with Ni clusters. Nickel was introduced into the cylindrical channels of the membrane via electro-deposition method. Then we washed out the polymer template with THF. The well ordered lattice of Ni dots of 15-20 nm in the diameter, 10 nm in the height with 25 nm in the period was observed with AFM (Fig. 7).

Taking into account the widening effect of AFM tip, the apparent size of the dots is in good agreement with the nano-template channel diameter (8 nm). Few defects (lacunas) appear in the array of Ni dots due to the non uniform electro-deposition kinetics of the metal clusters in nano-channels. Besides the potential application,

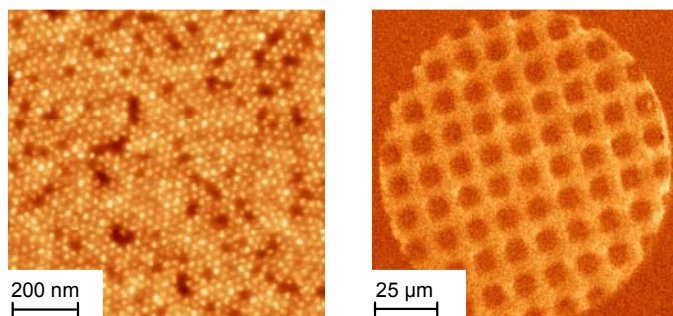


Fig. 7:  
Array of Ni dots loaded by electro-chemical deposition through BCA nano-template (left) and XPEEM images at Ni 2p peak of hierarchically ordered Ni array

this experiment gives evidence that the cylindrical channels cross the membrane from the top to the bottom.

Also, we performed Ni electro-deposition onto mosaic Cr electrode partially covered with insulating layer of poly(1,2-butadiene) (PBd). For that, thin film of PBD with addition of 5 % of photoinitiator, i.e. benzophenon, was spin-coated onto Cr covered wafer and illuminated with UV light (365 nm mercury lamp) through TEM grid of 12  $\mu\text{m}$  periodic square pattern. After washing with toluene, the 60 nm thick cross-linked PBD squares were revealed with large scale AFM. Micro-mapping ellipsometry showed that the shadowed location is free Cr surface. We deposited the SMA thin (70 nm) film on top of Cr mosaic electrode and completed it into nano-template with methanol rinse. Afterward, we performed Ni electro-deposition through the nano-template in galvanostatic direct current regime ( $0.3 \text{ mA}\cdot\text{cm}^{-2}$ , 1000 s) as described above and removed the polymer template in non-selective solvent (chloroform). Obtained samples were investigated with AFM and XPEEM.

The NEXAFS (near-edge X-ray absorption fine structure) measurements of Ni deposition were performed prior the XPEEM measurements to find the exact Ni 2p bonding energy as well as the peak width. The result of subtraction of XPEEM images before (851.5 eV) and after (854.0 eV) Ni 2p peak from the image required at the Ni 2p peak (853.0 eV) is shown in Fig. 7. It undoubtedly demonstrates distribution of Ni in the space between the PBd masked electrode surface. Thus, we obtained two scale hierarchy patterning combining electrode photolithography with insulating layer and nano-templating.

Another important example of application of BCA thin films as templates is deposition of electro-conductive polymers. We performed electro-deposition of polyaniline through BCA template. The result is shown on AFM image (Fig. 8).

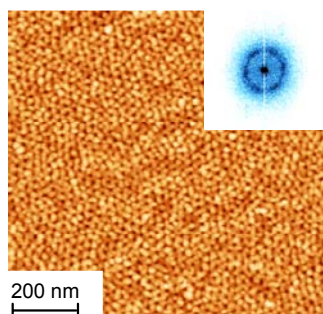


Fig. 8:  
AFM image of polyaniline deposited through BCA template

The details of kinetics of polyaniline deposition and electrical properties of obtained polyaniline nano-dots show clear difference with flat polyaniline layers. They are a subject of further investigations.

Nowadays, sputter-coating technique is widely used for deposition of various materials, such as metals, oxides, ceramics etc. We applied sputter-coating of Cr and Au onto surface of BCA templates in both  $C\parallel$  and  $C\perp$  orientation. The depositions resulted in formation of metal nano-wires or arrays of metal dots, respectively (Fig. 9).

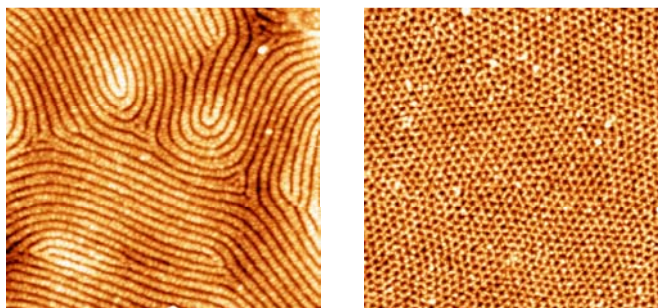


Fig. 9:  
Cr clusters sputtered onto nano-templates of parallel (top) and perpendicularly aligned cylinders. In all cases the nanotemplates are dissolved.

## Conclusions

The results obtained in the frame of the project are of sufficient interest for both fundamental science and applications. We have synthesized a novel class of materials with unique properties, i.e. block copolymer supramolecular assemblies and investigated their properties, such as selective formation of hydrogen bonds, micro-phase separation in bulk and in thin films, and the fine structure of the BCA. Moreover, we described a new phenomenon of solvent induced orientation and switching in thin films of BCA. We expect that this results might give an impulse to further fundamental investigations in this field.

We believe that block copolymer assembly approach opens a venue to fabricate polymer nanotemplates with ordered channels of nanometer scale periodicity. We demonstrated that loading of the nano-templates with functional species allows to obtain well-defined periodic arrays of nano-dots/nano-wires with specific properties. It is a subject of the further investigations to improve the loading procedures in respect to the quality of the nano-arrays and evaluate the impact of the nanometer feature size on the physical properties of the arrays. The results are of essential interest for number of applications, such as nano-technology, photonics, optoelectronics and others.

Major results have been published in several papers [8-10] and presented at numerous meetings, workshops and conferences.

## References

- [1] Whitesides, G.M.; Mathias, J.P.; Seto, C.T.: *Science* 254 (1991), pp 1312-1319
- [2] Whitesides, G.M.; Boncheva, M.: *Proc. Natl. Acad. Sci. USA* 99 (2002), pp 4769-4774
- [3] Bates, F.S.; Fredrickson, G.H.: *Annu. Rev. Phys. Chem.* 41 (1990), pp 525-557
- [4] Ruokolainen, J.; Saariaho, M.; Ikkala, O.T.; ten Brinke, G.; Thomas, E.L.; Torkkeli, M.; Serimaa, R.: *Macromolecules* 32 (1999), pp 1152-1158
- [5] Ruokolainen, J.; Ikkala, O.T.; ten Brinke, G.: *Adv. Mat.* 11 (1999), pp 777-780
- [6] Mäkinen, R.; Ruokolainen, J.; Ikkala, O.T.; de Moel, K.; ten Brinke, G.; De Odorico, W.; Stamm, M.: *Macromolecules* 33 (2000), pp 3441-3446
- [7] Mäki-Ontto, R.; de Moel, K.; De Odorico, W.; Ruokolainen, J.; Stamm, M.; ten Brinke, G.; Ikkala, O.T.: *Adv. Mat.* 13 (2001), pp 117-121
- [8] Sidorenko, A.; Tokarev, I.; Krenek, R.; Burkov, Y.; Schmeisser, D.; Minko, S.; Stamm, M.: *Generation of nanostructured materials from thin films of block copolymer assemblies.* – in: "Nanostructured Materials" / ed. H.J. Fecht, Wiley InterScience, Weinheim, ISBN: 3-527-31009-6 (2004)
- [9] Sidorenko, A.; Tokarev, I.; Minko, S.; Stamm, M.: *J. Am. Chem. Soc.* 125 (2003), pp 12211-12216
- [10] Tokarev, I.; Krenek, R.; Burkov, Y.; Schmeisser, D.; Sidorenko, A.; Minko, S.; Stamm, M.: *Macromolecules* 38 (2005) pp. 506-517